Real-Time Wearable Electrogoniometry System for Measuring Range of Motion in Rehabilitation Applications

Maurizio Pellegrini, *Graduate Student Member, IEEE*, Giuseppe Coviello, *Senior Member, IEEE*, Giuseppe Brunetti, *Associate Member, IEEE*, and Caterina Ciminelli, *Senior Member, IEEE*

***Abstract*—This article presents a wearable, low-cost, and high-accuracy electrogoniometry system designed for the dynamic measurement of range of motion (ROM). The system integrates two-axis capacitive flex sensors attached to the joints in both the upper and lower limbs (i.e., shoulder, elbow, hip, knee, ankle) through a modular, 3-D-printed framework. The electrogoniometry system aims to detect movement accurately for clinical purposes (e.g., evaluating the onset of diseases that affect mobility) and to control innovative treatment techniques such as precision electrical muscle stimulation (EMS) systems. Following ROM measurement guidelines, the system was successfully validated for accuracy by comparison with video-based motion capture (VMC) software across all aforementioned joints. The proposed system (PS) achieved root mean square error (RMSE) values below 4°, maximum ROM difference (MRD) below 2.5°, correlation coefficients of 99% or higher, and Bland–Altman analysis results of 0.644° ± 4.786°.**

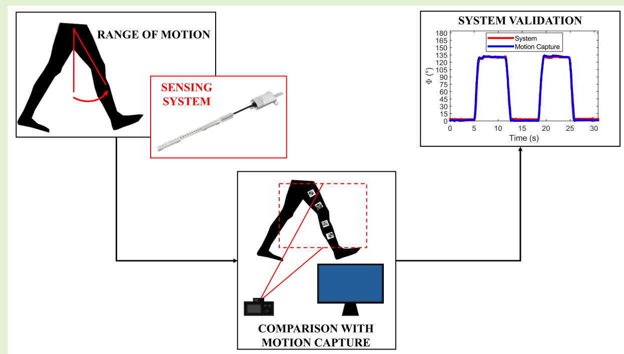

***Index Terms*—Biomedical monitoring, digital health, electrogoniometer, patient rehabilitation, range of motion (ROM), wearable sensors.**

I. Introduction

IN THE field of rehabilitation, the detection and tracking of movement of a patient is very important in analyzing the outcome of a given treatment following injury and the onset or progression of motor impairing diseases [1]. These latter pathologies can cause progressive damage to the musculoskeletal or neurological condition of the patient, altering either the muscles or the communication vias that lead to their activation [2]. Clinical care for these conditions can vary from the traditional hands-on approach from medical professionals to more cutting-edge treatments and may follow a patient starting from the Intensive Care Unit (ICU) all the way to at-home therapy.

Received 26 May 2025; revised 17 July 2025; accepted 17 July 2025. Date of publication 29 July 2025; date of current version 3 September 2025. The associate editor coordinating the review of this article and approving it for publication was Prof. Anindya Nag. *(Corresponding author: Caterina Ciminelli.)*

This work involved human subjects or animals in its research. The authors confirm that all human/animal subject research procedures and protocols are exempt from review board approval.

The authors are with the Optoelectronics Laboratory, Politecnico di Bari, 70126 Bari, Italy (e-mail: caterina.ciminelli@poliba.it).

Digital Object Identifier 10.1109/JSEN.2025.3592092

Innovative therapeutical approaches like functional electrical stimulation (FES) and neuro-muscular electrical stimulation (NMES) can help regain functionality in paralyzed patients and counteract atrophic conditions and consequent limitations in movement capabilities, respectively. This is by providing electrical pulses for the affected muscles helping, in both cases, to maintain or regain their strength and tone. Additionally, some may also be used without professional supervision facilitating the telemedical approach [3], [4], [5]. For all these active treatments, some form of biofeedback may enable precision rehabilitation adjusting stimulation based on the characteristics of a given movement [2]. Given these considerations, precise measurement of the range of motion (ROM) is clinically significant, highlighting the necessity of a reliable electrogoniometry system. ROM refers to the arc of motion between the initial and final positions of joint movement within a specific anatomical plane [1].

A wearable ROM measurement sensor, designed for applications such as those mentioned above, must possess specific capabilities to facilitate seamless integration into more complex and comprehensive systems. Key considerations include comfort, accuracy, and cost. The sensor should seamlessly integrate into the user's daily life, ensuring it is unobtrusive and comfortable to wear, thereby enabling continuous data collection during activities of daily livings (ADLs). Moreover, it must provide sufficient accuracy to be clinically relevant and to ensure the proper functioning of the broader system. Additionally, cost-effectiveness is crucial to extend its applicability beyond specialized medical facilities and clinics. Currently, the most widely used systems are highly dependent on the expertise of the medical personnel carrying out the examination and/or allow for only statistical measurements and not real-time measurements of the subject's ROM. This latter is essential to enable the continuous monitoring of treatment efficacy and adjustments during therapy needed for cutting-edge precision rehabilitation. In this area, wearable systems may also find use as feedback techniques for innovative robotics and prosthetics. In this regard, wearable motion tracking technologies have demonstrated significant potential for monitoring joint and muscle movements in dynamic environments.

Examples include its use in human activity recognition for adaptable assistance exoskeletons control [6], and gait motion monitoring of Parkinson's disease for movement reconstruction and body control assessment [7].

Application in extreme environments like space should also be considered as the exposure to microgravity causes muscle atrophy in major load-bearing muscles (e.g., quadriceps femoris, gastrocnemius, biceps brachii), like the above-mentioned motor impairing diseases [8]. This study stems from the need for precise angle measurements required in electrical muscle stimulation (EMS) applications on astronauts, similar to the one described in [9]. EMS, a term often used interchangeably with NMES, indicates treatment to maintain or strengthen muscle mass, which is usually applied to abled body individuals like athletes.

Here, we propose and validate a complete motion-tracking/ROM measurement system that is lightweight, comfortable, wearable, and modular (i.e., composed of interchangeable pieces of different lengths, making it adaptable to various subjects). The system is also designed for simple and effective integration into more complex frameworks, featuring low computational complexity and low latency. It enables real-time onboard analysis, making it highly suitable for integration, for example, into a wearable system for intelligent EMS applications with immediate feedback (Fig. 1).

The manuscript is structured with Section II, which presents the state of the art along with a discussion on the advantages and disadvantages of various wearable motion detection technologies. In Section III, the proposed system (PS) is described. Section IV explains the validation methods as well as the accuracy metrics used. In Section V, the experimental results are presented, highlighting this work's effectiveness. Finally, in Section VI, conclusions are given, and possible future research activities are proposed.

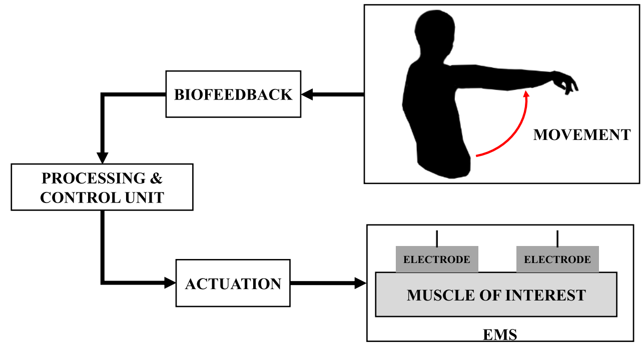

Fig. 1. Block diagram of an ROM measuring system usage as biofeedback in EMS application that may be used in cutting-edge rehabilitations procedures.

II. State of the Art

The most commonly used instrument for measuring ROM by medical professionals is the manual goniometer (either digital or analog). This instrument is, however, affected by errors depending on the expertise of the practitioner (e.g., alignment of the goniometer arms to the anatomical reference points). Additionally, the measured values are only applicable to clinical environments and are valid only for statistical measurements. These systems cannot, in fact, provide real-time and continuous assessment of the user's mobility condition. Also, it would be impossible to track end-to-end rotational motions or the angular speed of the executed movements [10].

The gold standard is represented by the video-based motion capture (VMC) and fluoroscopy systems. These systems can range in cost from 10000.00 \$ to 200000.00 \$ or more [1], [11]. Unfortunately, they suffer from errors given by the perspective of the recording camera which happens mostly in noncontrolled environments (e.g., parallax, camera angles, skin motion artifacts). These errors may cause up to 70% of posture misclassification compared to other technologies (i.e., electrogoniometers), as well as not being able to be used outside of specially designed environments. This, of course, does not favor the at-home approach or more dynamic settings because of the systems being immobile, hard to operate [12], [13], [14].

Wearable sensors offer a promising compromise between accuracy, low cost, and usage outside of specialized clinical settings. In fact, they allow for a truthful representation of the user's motor condition. They also enable reliable assessments of motor function in extreme environments where traditional manual or VMC technologies are impractical.

The most common wearables rely on Inertial Measurement Units (IMUs) or Inertial Magnetic Measurement Units (IMMUs), which are inexpensive, lightweight, easy to miniaturize, and wearable [15]. However, IMU and IMMU sensors are affected by errors caused by the intrinsic drift of gyroscopes (i.e., temperature shift), the skewing of magnetometers (i.e., external magnetic fields), and unwanted external accelerations on accelerometers (e.g., gait anomalies, scar, or adipose tissues) [14]. These errors may be mitigated via custom algorithms like sensor fusion techniques [14], [15], [16]. These methods combine the output of accelerometers, gyroscopes, and magnetometers present on IMUs or IMMUs to minimize the errors caused by the abovementioned problematics.

The Kalman filter and its variations are the most widely used techniques, though they require the inversion of large matrices. This increases computational complexity, processing time, and battery consumption. Simplifying these algorithms through linearization can reduce complexity but increases sensitivity to initial conditions and introduces linearization, truncation, and divergence errors [14], [17]. The high level of algorithm customization may limit the replication, introducing or exacerbating errors, and increase the cost of the systems [13], [15].

Computational complexity may also cause the need for a PC for processing, limiting the advantages of wearable sensors [14], [15]. Additional limitations are the low accuracy of the IMU systems at low rotational speeds (i.e., <10°/s) because of the lower strength of the inertial signal, and the high variance between methods of calibrations, significantly impacting the accuracy [10], [13].

An emerging technology in ROM measurements involves textile sensors that detect deformation and are used in wearable garments to achieve motion detection. As much as these systems are interesting and push the boundaries of biological measurement instrumentation, they are far from being commercialized and standardized enough to be able to continuously provide accurate ROM values for long durations of time. This, because they are still mostly lacking the necessary validations (e.g., comfort, structural strength, safety, efficiency, durability) [18].

Another technology is joint angle measurement from systems based on surface electromyography (sEMG). These however suffer from the same problems (e.g., movement artifacts, crosstalk, need of precise positioning over muscle groups) and need high computational cost to extrapolate ROM values from the sEMG signal [19], [20].

Fiber optic-based (FO) systems, on the other hand, are easily integrated into wearable garments and sensitive to deformation. Unfortunately, they usually provide only one degree of freedom of movement detection and need bulkier lab equipment (e.g., broadband light sources, optical spectrum analyzer, interrogators) which can impede on-board processing and full wearability. These systems typically use either Mach–Zender interferometers (MZIs) or fiber Bragg grating (FBG) [21], [22], [23].

Another option is the electrogoniometers, which provide an affordable alternative to gold standard systems for ROM measurement. These sensors detect movement by the measurement of angular displacement related to the change of resistance or capacitance of the flexible part [1]. Due to their computational simplicity, lightweight, flexibility-stretchability, and small dimensions, electrogoniometers can be easily integrated into sensors and actuators ecosystems as more than a VMC method.

In general, it is important to emphasize that a key aspect for the validation of these systems is that they will need an root mean square error (RMSE) lower than 5° to be considered acceptable for clinical evaluations of ROM-affecting pathologies, with errors <2° considered excellent. However, this threshold may vary depending on the specific case [15], [24]. For the control of an EMS system, some studies apply the same acceptability criterion, which should be sufficient to ensure proper adaptive stimulation [25]. Hence, we propose a system that incorporates an efficient and easy-to-integrate design and accuracy within the abovementioned acceptability ranges. Additionally, the PS has already been successfully tested in extreme environments, such as space in the Axiom Ax-3 mission, which concluded on the 9 February 2024, where it was tested during the 36 h of free flight in the SpaceX Crew Dragon [9].

III. System Description

The custom hardware developed is composed of an electronic control unit (ECU) that uses a 32-bit microcontroller to control the EMS by using the ROM data and two SD cards for continuous storage of the latter. The board can deliver current pulses to the target muscles with a magnitude of ±50 mA, and an adjustable frequency of 5–50 Hz with a minimum pulse duration of 250 μs across six channels. Further details are reported in [9].

The integrated sensors for ROM measurements are managed by two IIC buses, one on the right side and one on the left. This protocol was chosen to expand the number of measurement nodes without changing the overall architecture of the system. At this moment, the system does not implement wireless data transmission; however, this may be implemented in future to tailor the system to applications differing from health monitoring in astronauts, where wired data transfer is preferred. Information is provided through a miniaturized *LC* display, and the system is powered by an 18 650 battery, [9]. The dimensions of the ECU are tailored to the specific EMS application. If used solely for motion detection and ROM measurement, further miniaturization of the board would have been feasible.

The proposed electrogoniometry system, integrated into the abovementioned smart garment, utilizes as a sensor element a capacitive 2-axis soft flex sensor by Bend Labs which exhibits linear response in a range between ±105°. The sensor has a differential capacitance that varies from circa −3 to 6 pF and a standard deviation of ±0.25° in its linearity range. Furthermore, it has a repeatability of 0.18° and an average sensitivity of 0.274 pF/°. While the overall system accuracy depends on that of the sensor, this parameter will be evaluated and presented in the following sections. The sensor calculates the angle at which its tip is bent in relation to its base. This angle measurement is obtained from a differential capacitance measurement which is related to its degree of flexion by a linear relationship. This allows for a very versatile measurement, requiring only consideration of the orientation of the aforementioned measurement poles [26]. However, to accurately relate the sensing element output to a given joint angle, a specialized structure is required to ensure that the sensor remains consistently aligned with the joint's movement while minimizing orientation divergence as described below.

The sensing element, encased within the structure, is subsequently connected to the ECU, where the raw data are stored and later transferred to a PC for further processing. This step has been carried out solely for validation purposes by comparing the data with VMC results.

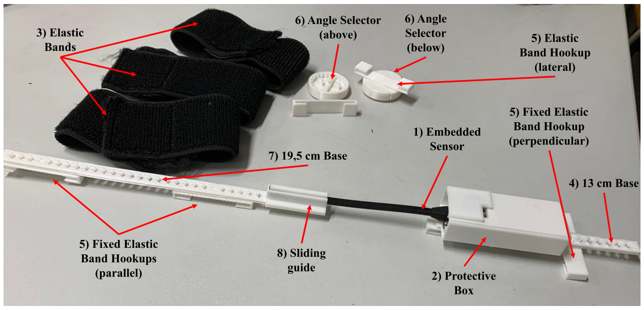

Fig. 2. PS composed of three elastic bands for fixture on the limb of the patient, two rigid bases to be blocked on the distal and proximal part of the joint, the sensing element encased in a protective box with its based blocked to the proximal rigid base, the sliding guide that allows the smooth movement of the tip of the sensor during bending, the angle selectors used for one-elastic band measurements only.

The raw data consist of the angle in degrees, at which the sensing element is bent. The relative ROM value is calculated as the difference between the maximum angle detected by the system and the zero-position obtained by the calibration procedure, which will be explained in Section IV. Additionally, raw data are filtered in real time by a ten-sample moving average filter and a 30 Hz, fourth order, FIR low-pass filter for effective stabilization of the output and the filtering of unwanted high-frequency noise.

The low-pass filter cutoff frequency has been chosen based on the maximum frequency of human motion which is 20 Hz.

The modular rigid structure that houses the sensor (Fig. 2 component 1) has been 3-D-printed in polylactic acid (PLA).

A box (7.40 × 1.86 × 3.30 cm) (Fig. 2 component 2) is designed to protect, block, and orient the sensor's base, fixing it to an adjustable elastic band (Fig. 2 component 3). This first structure, referred to as the proximal module, also includes a base that shows a width of 1.05 cm and a length of 6.50 or 13 cm (Fig. 2 component 4). Each base has a number of evenly spaced cross-shaped holes, enabling the attachment of additional modules and lateral rails for connecting 3-D-printed components. The base length is selected based on the joint being analyzed, with a longer base allowing for greater accuracy and comfort on longer joints by providing more distance between modules (e.g., facilitating placement on flatter, more stable body surfaces). The lateral rails allow for mounting the protective box.

The housing for the sensor's base is connected to the cross-shaped holes, in addition to either two elastic band hookups (Fig. 2 component 5) or an angle selector (Fig. 2 component 6) that allows for orientation change with a step of about 16.35°. These last two modules may only be useful when placing the system by hand with the use of elastic bands to study the possible effects of wrong positioning, and not when directly integrated into smart garments.

The distal structure is instead designed to be applied to the moving segment of the joint under analysis to allow for the guiding of the tip with the movement. This segment shows a 19 cm long base (Fig. 2 component 7), connected to the same number of hookups or angle selectors. The longer base is used for movements requiring a greater ROM.

The sliding tip (Fig. 2 component 8) is attached, via the side rails, to the base and completely blocks the sensor's tip and is then closed by a removable sliding lid. The rails are then blocked at the start of the base to impede the guide from sliding off, affecting the measure.

Hence, the developed system architecture allows for measurements with the following characteristics.

1) *Versatility:* The system can function in a much more complex environment, providing accurate ROM measurements for various joints in both the upper and lower limbs. During testing, this configuration (i.e., using elastic bands) allows for a preliminary study of the PS positioning on the user's body before the integration in a sensorized garment.
2) *Comfort:* The only parts in contact with the skin of the user are the flexible and adjustable elastic bands, with the other rigid PLA modules being separated and positioned parallel to the patient's limbs or torso. In future, it could be directly integrated into comfortable and easy-to-wear smart garments.
3) *Fast Response:* Because of its low computational complexity, the system allows for 100 Hz angle measurements without requiring complex or additional filtering by the microcontroller. This is because the sensing element output is based on a differential capacitance measurement, which minimizes the effects of common mode noise.
4) *Low Cost:* The system utilizes hardware at much lower costs than the state-of-the-art goniometry technologies and 3-D printed elements, achieving high reusability, also given that the same architecture can be applied to multiple joints.
5) *High Parallelism:* The system provides simultaneous ROM measurements alongside additional functions like FES.
6) *Functionality:* The architecture allows for both online and offline analysis for daily use and long-term periods.

IV. Methods of Validation and Processing

The system has been tested through both dynamic and static experiments. In the static test, the prototype was mounted onto a digital goniometer (Parkside IAN 364969_2204) [27] completely isolating a single DOF eliminating mixed-plane artifacts [28]. In this in vitro testing session, eight measurements have been taken across a range of 15°–125°. The average error is 0.442°, and the maximum standard deviation is 0.419°. In the second phase, the prototype was worn on the elbow, and its measured ROM values compared with those of the same digital goniometer, achieving a total mean error of 1.401° and a maximum standard deviation of 1.850° (i.e., eight measures from 15° to maximum ROM). Dynamic testing consists of a minute and a half of walking and results in a measurement of an average ROM of 29.841°, consistent with values reported in the literature.

To complete the validation of the whole PS's performance, the accuracy has been tested by calculating the ROM of multiple joints on both the upper and lower limbs (i.e., elbow, shoulder, hip, knee, and ankle). Given the nature of the tested joints, the shoulder, the hip, and the ankle have been tested for both the flexion-extension (f-e) and adduction-abduction (ad-ab) movements, taking advantage of the 2 DOF nature of the PS. Given their nature, both the elbow and the knee have been tested only for the 1 DOF flexion extension.

By definition, f-e is a movement that causes, respectively, a decrease or increase in the angle between the distal and proximal segment of a joint [29].

Ad-ab is defined as a movement that causes, respectively, a decrease or an increase in the angle between the distal segment and the midsagittal plane (i.e., plane that cuts the center of the body in half when viewed from the front) [29].

The PS has been compared in real time to the VMC analysis of the abovementioned movements.

The VMC analysis utilizes the open-source video analysis and modeling tool tracker (Open Physics [30] and can acquire video at 60 fps and a resolution of 1920 × 1080 p.

For this analysis, markers have been placed at anatomical reference points, following the procedure outlined in [1], with the minimum ROM considered as the zero point. Four markers have been used in total: two on the distal and two on the proximal segment of the joint. The VMC system thus uses a joint-local coordinate system, because only one DOF has been recorded at a time for a more precise and in-depth comparison between the systems.

The electrogoniometry system has been aligned to match the imaginary lines formed between these markers and has been calibrated to 0° to ensure that only positive values would have been recorded, simplifying the comparison with VMC data. The testing procedure consisted of two repetitions with five seconds of rest in the starting position and 5 s holding at maximum ROM. For synchronization of the two measuring systems, an initial movement of circa half a ROM was carried out with a pause of about 5 s before the two main movement repetitions. The instant in which the movement started was thus considered as the synchronization point.

All the movements were carried out while the volunteer was in a prone position, within the camera's field of view.

The camera, mounted on a tripod (Fig. 3), has been oriented with its plane of view perpendicular to the ground via level and parallel to the wall in front, where two straight markings have been drawn, which have been used for alignment. The mattress, where the subject had to lie down, was then positioned parallel to the same wall. During movement, to maintain the desired orientation of the limb, clinical procedures have been followed to isolate as much as possible every DOF of movement [1], allowing for only the movement in the plane parallel to the camera to take place. Furthermore, the subject has been allowed to move only one joint at a time with the rest of the body posed in a stable position, and an operator verified if the movement would have been performed at an acceptable angle to the recording plane.

The volunteer for this validation procedure was of 24 years of age, male, 1.83 m tall, healthy and in good physical condition.

An exception to this setup has been made for ankle adduction-abduction movement, where the volunteer had to be seated to achieve full ROM. In this case, the volunteer sat

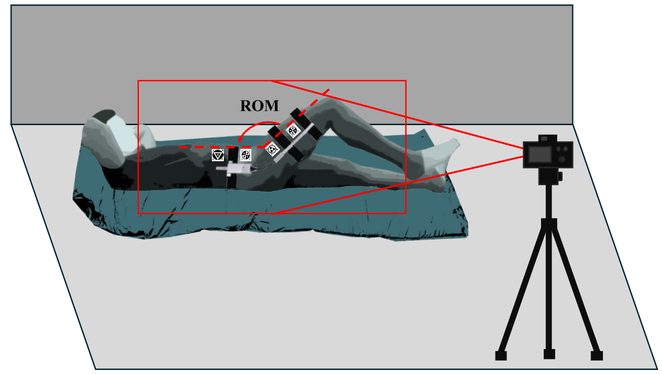

Fig. 3. VMC setup used for the comparison with the PS, where the subject lies down on a mattress parallel to the wall in shot of the camera with makers clearly visible.

on a chair positioned with the same precautions applied to the mattress. The data extracted from both measurement methods have been then exported to MATLAB for processing. Temporal alignment has been performed for an effective comparison of the two datasets.

To validate the PS's accuracy, the following metrics have been derived.

1) RMSE, which has been used as a metric of point-to-point accuracy between the proposed and reference systems.
2) Maximum ROM Difference (MRD), which has been considered as the difference between the maximum values measured ROM of the proposed and reference systems. This is important as this value may clinically verify the presence of movement-affecting pathologies by quantifying the maximum possible movement of one joint.
3) Correlation coefficient, which is the linear dependence of the two compared signal distributions, has been used as a measure of similarity.
4) Bland–Altman analysis, which indicates the mean absolute error (MAE) ± 1.96 times the standard deviation and is a measure of agreement between two measurement systems or techniques indicating bias and the limits of agreement (LOA).

V. Experimental Results

The results of the comparison between the PS and the VMC software analysis are summarized in Table I and shown in Fig. 4, highlighting the performance and reliability of the system across various movement types.

In general, it has been observed that asperities on the surfaces of the body may marginally affect the measurements, and this may have influenced the decrease in correlation in the adduction-abduction of the ankle joint (i.e., 99%), which is the lowest measured. The same could be said for the flexion-extension of the hip.

It can be therefore deduced that the system has been observed to achieve better results when positioned on flatter surfaces that are not deformed during the measured movement, including the belly of muscles like the biceps brachii, or the quadriceps femoris (mostly for the proximal module), and

TABLE I
ROM COMPARISON ANALYSIS

Joints	ROM comparison metrics			
	RMSE	*MRD (max PS – max MC)*	*Correlation*	*Bland-Altman*
Ankle f-e (A. f-e)	1.363°	0.136° (46.344° - 46.479°)	99.8%	0.029° ± 2.672°
Ankle ad-ab (A. ad-ab)	2.373°	1.792° (29.092° - 30.855°)	99.0%	0.932° ± 4.279°
Knee f-e (K. f-e)	3.756°	2.492° (122.312° - 124.804°)	99.8%	0.188° ± 7.353°
Hip f-e (H. f-e)	3.882°	1.332° (108.594° - 109.925°)	99.8%	2.342° ± 6.070°
Hip ad-ab (H. ad-ab)	2.725°	0.368° (69.625° - 69.257°)	99.7%	0.426° ± 5.277°
Elbow f-e (E. f-e)	3.696°	0.669° (135.906° - 135.237°)	99.8%	0.370° ± 7.210°
Shoulder horizontal f-e (S. h. f-e)	3.232°	0.713° (122.000° - 122.713°)	99.8%	0.055° ± 6.335°
Shoulder ad-ab (S. ad-ab)	3.216°	1.348° (132.656° - 134.004°)	99.9%	0.814° ± 6.302°

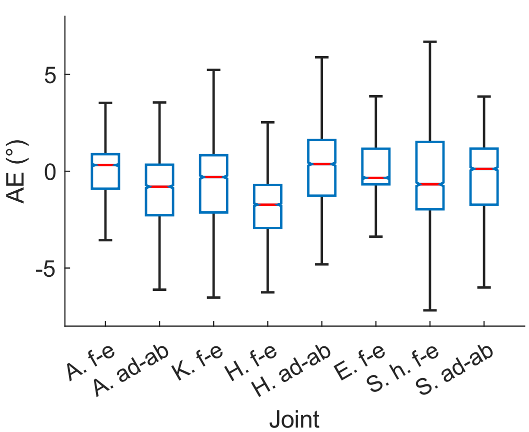

Fig. 4. Boxplot of the AE distribution in the ankle for all the carried-out movements of the tested joints, where low variability of the absolute error between the synchronized data points from the PS and the VMC reference. The mean (red line) is close to 0° and the standard deviations (black lines) are all under the range of ±7.5°.

bony regions like the forearm or the tibia (mostly for the distal module).

In the case of the knee, the presence of both the quadriceps femoris and the calf may have contributed to the shifting of the PS. Furthermore, placing the two modules farther apart caused a minor detriment in accuracy because the two segments may pull on each other, causing divergence from the desired measuring orientation.

From the captured video, it has been possible to notice that these last two points are what may have influenced the slight loss in accuracy observed in the knee flexion-extension movement, where higher RMSE and MRD values have been observed. Such is the case of the shoulder horizontal flexion-extension movement where the proximal module has been placed on the pectoral of the subject and the distal on the biceps brachii. All the aforementioned sources of error may vary in significance depending on the tested joint, as each has a distinct anatomy. However, their overall impact on the results has been minimal. For example, during the f-e of the ankle, a fairer surface has been encountered and resulted in lower errors than the same movement measured on the hip. To achieve even better results than the ones already presented in the manuscript, these problems would need to be addressed. Differently for what has been seen for surface asperities, different characteristics in skin-sensor contact that may affect measures in other technologies, causing the relative movement of the sensor in relation to the bone [31], are not impacting on the PS. This is because the utilized sensing element is independent of the path undertaken by its flexible part, minimizing any errors caused by skin-bone relative movements, as long as the base and the tip are properly fixed to the limb.

In future, the development of more adaptable calibration procedures could actively compensate for the effects of surface asperities. The boxplot of the AE distribution values for all the tested joints and carried-out movements can be observed in Fig. 4, where the measured AEs demonstrate very low variability, complementing the results already shown in Table I.

Overall, the PS achieved optimal results, demonstrating excellent precision in detecting the user's movements. Of all the observed results, of particular interest are the flexion extension of the ankle joint where the lowest RMSE and MRD have been observed and the shoulder adduction-abduction movement that achieved the highest recorded correlation of 99.9%. Hence, the system's ability to accurately capture and interpret motion data highlights its effectiveness in various applications.

These findings stress the robustness of the system, reinforcing its potential for reliable use in applications where precise movement tracking is crucial. The strong results from this evaluation suggest that the system can reliably meet user demands for high-fidelity motion detection.

Table II reports the comparison between our findings with the state of the art by using the same metrics.

All the values have been averaged between the results over all the joints to allow for a more direct comparison, and the standard deviations reflect the metrics'variability between the joints. For the Bland–Altman analysis, the standard deviation is calculated as the mean, across all joints, of those shown in Table I. However, since not all metrics are reported in every article, we included those that have been explicitly provided or those that we have been able to derive from the available results.

Furthermore, we added the following metrics for comparison.

1) Modularity (i.e., systems that are composed of interchangeable pieces and can be adapted to different joints are considered modular).
2) Edge computing (i.e., complete wearability is achieved when there is no need for external computation: full on-board processing).

TABLE II
RELATED WORKS COMPARISON (DESIGN AND RESULTS)

Works	Technology	Modularity	Edge Computing	Computational cost	Test type	Analyzed Joints (**)	DOF	RMSE	MAE	Mean Correlation	Bland-Altman
This work	Capacitive Sensor	Yes	Yes	Low	Dynamic	E, S, H, K, A	2 (F-E, Ab-Ad)	3.03° ± 0.85°	0.644° ± 0.7607°	99.7%	0.644° ± 4.786°
[10]	Gyroscope	No	No	-	Static	E, S (Non-simultaneous)	3 (F-E, Ad-Ab, InR-ExR)	-	2.52° (*)	-	-
[14]	MIMU	Yes	Yes	Low	Dynamic	H, K, E	1 (F-E)	2.5°	-	95.1%	-
[15]	IMU	Yes	Yes	Very High	Dynamic	W, E, S, T, H, K, A	3 (F-E, Ab-Ad, InR-ExR)	5° (*)	-	93.61% (*)	-
[16]	Hall Effect Sensor	Yes	No	Low	Static	K	1 (F-E)	-	7.475° ± 4.56° (*)	-	-
[17]	MIMU	Yes	No	-	Dynamic	S	3 (F-E, Ab, InR-ExR)	2.92° ± 1.302° (*)	-	-	-
[19]	sEMG	Yes	No	High	Dynamic	H, K	1 (F-E)	0.32°	20.23°		-
[20]	IMU	Yes	Yes	-	Dynamic	K	1 (F-E)	2.61°	-	98%	1,26° ± 4.34° (*)
[21]	FBG (FO)	Yes	No	-	Static	E	1 (F-E)	-	-	99.5%	-
[22]	MZI (FO)	Yes	No	-	Static	K	1 (F-E)	-	-	99.8%	-
[23]	FBG (FO)	No	No	-	Static	E, K	1 (F-E)	-	9.5% (E), Not mentioned (K)	99.34% (*)	-
[32]	Capacitive Sensor	No	No	-	Dynamic	K	1 (F-E)	5.582°	4.429°	96.97% (*)	-
[33]	Textile	Yes	No	Low	Dynamic	K	1 (F-E)	12.17°	10.68°	-	3.33° ± 22.04° (*)
[34]	IMU	No	No	-	Static	W	2 (F-E, InR-ExR)	-	< 2°	-	-
[35]	Magnetic Rotary Encoders	No	No	Low	Dynamic	W, E, S	3 (F-E, Ab-Ad, InR-ExR)	5.32° ± 1.26° (*)	-	> 90%	3.40° ± 21.85° (*)
[36]	Resistive Strain Sensor	Yes	Yes	Low	Dynamic	K	1 (F-E)	-	-	-	0.96° ± 27.07°
[37]	sEMG	Yes	No	-	Dynamic	W	1 (F-E)	12.80° ± 3.60° (*)	-	96.94% (*)	-
[38]	sEMG	No	No	High	Dynamic	E	1 (F-E)	0.27°	9.7588°	98.25%	3,5° ± 21.7° (*)
[39]	Potentiometer	Yes	-	-	Dynamic	K	1 (F-E)	5.0° ± 1.0°	3.9° ± 0.8°	96.95% (*)	-

(*) Values have been obtained from the results presented in the referenced articles. (**) Abbreviations: wrist (W), elbow (E), shoulder (S), torso (T), hip (H), knee (K), ankle (A), internal rotation-external rotation (InR-ExR), flexion-extension (F-E), abduction-adduction (Ab-Ad).

3) Computational cost (i.e., systems that obtained ROM values in real time, with low latencies and without relying on external computational platforms).
4) Test type, either dynamic or static (i.e., a test is considered dynamic if a comparison between the trend of the movement captured with the proposed and reference system can be traced; else it is considered static).
5) Joint under analysis (i.e., the joint on which the PS has been tested).
6) Degrees of freedom or detectable movements.

As it is possible to observe, from the gathered literature data, although most systems are modular in nature, they don't include on-board processing (i.e., edge computing), which limits applicability outside of laboratory use.

Additionally, some of the systems also presented limits regarding the latencies of the measurement, making use of high computational cost algorithms that will also limit their applicability for real-time ROM measurement and control of actuators (e.g., intelligent EMS, robotics). Some works also validated their systems with only a static analysis, which makes it impossible to evaluate if it would capture a movement in its entirety, allowing for a correct reproduction. Moreover, most of the related works only validated their function on one joint and for only 1 DOF movement detection.

In terms of raw quantitative metrics, we may observe that our system achieves a mean RMSE comparable to those of the related systems, with a much lower MAE and the second-highest correlation. From the Bland–Altman analysis, it can also be gathered that the PS has very high agreement with the measurements of the reference system.

Hence, from this analysis, the capabilities of the PS are highlighted, not only for its accuracy and agreement with the reference system but also for its ability to be used on multiple joints with low latencies and the possibility of on-board processing, making it adaptable to different subjects and environments.

VI. Conclusion

The proposed wearable electrogoniometry system has demonstrated highly promising performance, achieving RMSE values lower than 4° and MRD values below 2.5° across all tested joints. MAE values are all inferior to 2.4° with LOAs under 7.5°, as gathered from the Bland–Altman analysis. Furthermore, the correlation between the PS and the VMC software has been consistently 99% or higher, ensuring optimal capture of the wearer's movements. These results confirm the system's potential not only as a control mechanism but also as a precise clinical tool.

The PS's measurement capabilities also fall in the already mentioned range of acceptability for clinical ROM measures and EMS systems'control (i.e., RMSE $< 5°$). The system's easy integration into more complex environments (such as intelligent EMS systems, prosthetic controls, telemedicine platforms, and IoT networks), without adding unnecessary complexity, underscores its versatility. The system also enables 3-D reconstruction of the user's movements, providing a valuable tool for motion tracking and analysis. This capability lends itself to a variety of applications, including rehabilitation, exercise monitoring, and astronaut training. It enables medical personnel to accurately assess movement quality, optimize exercise protocols—both on Earth and in microgravity conditions—and prevent injuries caused by improper execution.

Direct integration of the whole system in wearable garments will also be explored to allow for even quicker dress-on, dress-off times of the electrogoniometer. This may also heighten the accuracy and repeatability of the measures by adding anatomical reference points on the sensorized clothes to allow for more precise positioning of both the proximal and distal modules.

Future developments will aim to extend the system to wrist and hand joints, enabling a more complete musculoskeletal analysis. To achieve this step, challenges would need to be faced, especially those associated with the PS miniaturization and to the more complex positioning analysis that would need to be carried out to effectively measure ROM values without impeding movement. This is because of the higher concentration of joints and degrees of freedom, especially when considering the fingers. Implementing data fusion from multiple joints to generate aggregated metrics for enhanced movement evaluation also represents an interesting future development. Additionally, the usage of the PS's motion tracking capability in conjunction with machine learning for movement recognition may also be explored. The PS will also be tested, given the possibility, on elderly and physically impaired individuals to help with generalization of the results, also allowing to consider for participant diversity and anatomical variance which is currently a limitation of our work.

References

[1] C. C. Norkin and D. J. White, *Measurement of Joint Motion: A Guide to Goniometry*, 5th ed., Philadelphia, PA, USA: F.A Davis Company, 2016.

[2] R. R. Saxena, R. Saxena, and A. Patel, "Functional electrical stimulation as a significant bioelectronic intervention in the domain of fitness: A review," *FMDB Trans. Sustain. Energy Sequence*, vol. 1, no. 2, pp. 94–106, 2023.

[3] J. Edwards, D. McWilliams, M. Thomas, and S. Shah, "Electrical muscle stimulation in the intensive care unit: An integrative review," *J. Intensive Care Soc.*, vol. 15, no. 2, pp. 142–149, Apr. 2014.

[4] P. H. Peckham and J. S. Knutson, "Functional electrical stimulation for neuromuscular applications," *Annu. Rev. Biomed. Eng.*, vol. 7, no. 1, pp. 327–359, Aug. 2005.

[5] J. S. Knutson, N. S. Makowski, K. L. Kilgore, and J. Chae, "Neuromuscular electrical stimulation applications," in *Atlas Orthoses Assistive Devices*, vol. 43, 5th ed., Philadelphia, PA, USA: Elsevier, 2019, pp. 432–439.

[6] D. Martínez-Pascual, J. M. Catalán, A. Blanco-Ivorra, M. Sanchís, F. Arán-Ais, and N. García-Aracil, "Gait activity classification with convolutional neural network using lower limb angle measurement from inertial sensors," *IEEE Sensors J.*, vol. 24, no. 13, pp. 21479–21489, Jul. 2024.

[7] R. Liu et al., "Quantitative analysis of lower limb motion in Parkinson's disease based on inertial sensors," *IEEE Sensors J.*, vol. 22, no. 21, pp. 20937–20946, Nov. 2022.

[8] N. Nguyen, G. Kim, and K.-S. Kim, "Effects of microgravity on human physiology," *Korean J. Aerosp. Environ. Med.*, vol. 30, no. 1, pp. 25–29, Apr. 2020.

[9] M. Pellegrini et al., "Design and development of new wearable and protective equipment for human spaceflights," in *Proc. Int. Conf. Appl. Electron. Pervading Ind., Environ. Soc.*, 2024, pp. 189–195.

[10] V. Chandel, M. Poduval, and A. Ghose, "ROMeasure: A practical solution for accurate range of motion analysis using a smartwatch," in *Proc. IEEE Int. Conf. Pervasive Comput. Commun. Workshops other Affiliated Events (PerCom Workshops)*, Pisa, Italy, Mar. 2022, pp. 806–811.

[11] R. M. Chapman, W. E. Moschetti, and D. W. Van Citters, "Is clinically measured knee range of motion after total knee arthroplasty 'good enough': A feasibility study using wearable inertial measurement units to compare knee range of motion captured during physical therapy versus at home," *Med. Novel Technol. Devices*, vol. 11, Sep. 2021, Art. no. 100085.

[12] C. D. McKinnon, S. Ehmke, A. M. Kociolek, J. P. Callaghan, and P. J. Keir, "Wrist posture estimation differences and reliability between video analysis and electrogoniometer methods," *Hum. Factors, J. Hum. Factors Ergonom. Soc.*, vol. 63, no. 7, pp. 1284–1294, Nov. 2021.

[13] C. P. Walmsley, S. A. Williams, T. Grisbrook, C. Elliott, C. Imms, and A. Campbell, "Measurement of upper limb range of motion using wearable sensors: A systematic review," *Sports Med. Open*, vol. 4, no. 1, p. 53, Dec. 2018.

[14] S. Majumder and M. J. Deen, "Wearable IMU-based system for real-time monitoring of lower-limb joints," *IEEE Sensors J.*, vol. 21, no. 6, pp. 8267–8275, Mar. 2021.

[15] P. Slade, A. Habib, J. L. Hicks, and S. L. Delp, "An open-source and wearable system for measuring 3D human motion in real-time," *IEEE Trans. Biomed. Eng.*, vol. 69, no. 2, pp. 678–688, Feb. 2022.

[16] B. Rivera, C. Cano, I. Luis, and D. A. Elias, "A 3D-printed knee wearable goniometer with a mobile-app interface for measuring range of motion and monitoring activities," *Sensors*, vol. 22, no. 3, pp. 763–777, Jan. 2022.

[17] Y.-C. Lin, Y.-J. Tsai, Y.-L. Hsu, M.-H. Yen, and J.-S. Wang, "Assessment of shoulder range of motion using a wearable inertial sensor network," *IEEE Sensors J.*, vol. 21, no. 13, pp. 15330–15341, Jul. 2021.

[18] I. I. Shuvo, A. Shah, and C. Dagdeviren, "Electronic textile sensors for decoding vital body signals: State-of-the-art review on characterizations and recommendations," *Adv. Intell. Syst.*, vol. 4, no. 4, Apr. 2022, Art. no. 2100223.

[19] P. Qin and X. Shi, "A novel method for lower limb joint angle estimation based on sEMG signal," *IEEE Trans. Instrum. Meas.*, vol. 70, pp. 1–9, 2021.

[20] R.-U. Nissa, N. C. Karmakar, and M. S. Baghini, "A wearable accelerometer-based system for knee angle monitoring during physiotherapy," *IEEE Sensors J.*, vol. 24, no. 13, pp. 21417–21425, Jul. 2024.

[21] S. Gao, S. Ma, Y. Xu, H. Wu, and Q. Wang, "Application and optimization of distributed fiber grating-based flexible wearable sensors in the shooting sports," *IEEE Trans. Instrum. Meas.*, vol. 73, pp. 1–8, 2024.

[22] X. Zhu et al., "A novel wearable knee joint angle monitoring sensor utilizing Mach–Zehnder interferometer with triple-clad fiber," *IEEE Sensor J.*, vol. 24, no. 3, pp. 2785–2791, Dec. 2023.

[23] H. Cheng-Yu, Z. A. Abro, Z. Yi-Fan, and R. A. Lakho, "An FBG-based smart wearable ring fabricated using FDM for monitoring body joint motion," *J. Ind. Textiles*, vol. 50, no. 10, pp. 1660–1673, Jun. 2021.

[24] J. L. McGinley, R. Baker, R. Wolfe, and M. E. Morris, "The reliability of three-dimensional kinematic gait measurements: A systematic review," *Gait Posture*, vol. 29, no. 3, pp. 360–369, Apr. 2009.

[25] F. Feuvrier et al., "Inertial measurement unit compared to an optical motion capturing system in post-stroke individuals with foot-drop syndrome," *Ann. Phys. Rehabil. Med.*, vol. 63, no. 3, pp. 195–201, May 2020.

[26] Nitto.com. (2022). *2-Axis Evaluation Kit-Nitto Bend Technologies*. Accessed: Feb. 15, 2024. [Online]. Available: https://www.nitto.com/eu/en/nbt/products/2-axis-evaluation-kit/

[27] M. Pellegrini, G. Coviello, G. Brunetti, F. Angelini, F. A. Gentile, and C. Ciminelli, "Low-cost limb flexion assessment: Integrating muscle stimulation and electrogoniometry in rehabilitation," in *Proc. IEEE Int. Symp. Med. Meas. Appl. (MeMeA)*, Eindhoven, The Netherlands, Jun. 2024, pp. 1–5.

[28] S. Mihcin, "Simultaneous validation of wearable motion capture system for lower body applications: Over single plane range of motion (ROM) and gait activities," *Biomed. Eng./Biomedizinische Technik*, vol. 67, no. 3, pp. 185–199, Jun. 2022.

[29] R. Hartline, *Human Anatomy Laboratory Manual*. Lemoore, CA, USA: LibreTexts, West Hills College Lemoore, 2020.

[30] Open Source Physics. (2024). *Tracker Video Analysis and Modelling Tool*. Accessed: Jul. 30, 2024. [Online]. Available: https://physlets.org/tracker/

[31] S. Mihcin, "Methodology on co-registration of MRI and optoelectronic motion capture marker sets: In-vivo wrist case study," *Hittite J. Sci. Eng.*, vol. 6, no. 2, pp. 99–107, 2019.

[32] L. Feng et al., "Locomotion joint angle and moment estimation with soft wearable sensors for personalized exosuit control," *IEEE Trans. Neural Syst. Rehabil. Eng.*, vol. 33, pp. 1048–1060, 2025.

[33] J. Di Tocco et al., "Wearable device based on a flexible conductive textile for knee joint movements monitoring," *IEEE Sensors J.*, vol. 21, no. 23, pp. 26655–26664, Dec. 2021.

[34] F. Engstrand, E. Tesselaar, R. Gestblom, and S. Farnebo, "Validation of a smartphone application and wearable sensor for measurements of wrist motions," *J. Hand Surgery (Eur. Volume)*, vol. 46, no. 10, pp. 1057–1063, Dec. 2021.

[35] A. C. De Oliveira, J. S. Sulzer, and A. D. Deshpande, "Assessment of upper-extremity joint angles using harmony exoskeleton," *IEEE Trans. Neural Syst. Rehabil. Eng.*, vol. 29, pp. 916–925, 2021.

[36] H.-B. Choi et al., "Concurrent validity of wearable nanocomposite strain sensor with two-dimensional goniometer and its reliability for monitoring knee active range of motion in multiple participants," *IEEE Trans. Neural Syst. Rehabil. Eng.*, vol. 32, pp. 4314–4321, 2024.

[37] Y. Zhao, Z. Zhang, Z. Li, Z. Yang, A. A. Dehghani-Sanij, and S. Xie, "An EMG-driven musculoskeletal model for estimating continuous wrist motion," *IEEE Trans. Neural Syst. Rehabil. Eng.*, vol. 28, no. 12, pp. 3113–3120, Dec. 2020.

[38] H. Li, S. Guo, H. Wang, and D. Bu, "Subject-independent continuous estimation of sEMG-based joint angles using both multisource domain adaptation and BP neural network," *IEEE Trans. Instrum. Meas.*, vol. 72, 2023, Art. no. 4000910.

[39] B. Oubre et al., "A simple low-cost wearable sensor for long-term ambulatory monitoring of knee joint kinematics," *IEEE Trans. Biomed. Eng.*, vol. 67, no. 12, pp. 3483–3490, Dec. 2020.

Maurizio Pellegrini (Graduate Student Member, IEEE) received the bachelor's degree and the master's degree in medical systems engineering from the Politecnico di Bari, Bari, Italy, in 2022 and 2023 respectively.

In November 2023, he started a Ph.D. program in aerospace sciences and engineering at the Politecnico di Bari. His research interests include health monitoring technologies for astronauts during space missions and for civilian healthcare.

Giuseppe Coviello (Senior Member, IEEE) was born in Bari, Italy, in 1981. He received the Laurea degree in electronic engineering and the Ph.D. degree in electric and information engineering from the Polytechnic University of Bari, Bari, Italy, in 2006 and 2015, respectively.

He is currently an Assistant Professor with the Department of Electrical and Information Engineering, Polytechnic University of Bari. His research interests include RF and mixed-signal circuits and embedded systems for healthcare.

Giuseppe Brunetti (Associate Member, IEEE) received the M.Sc. degree in electronic engineering (cum laude) and the Ph.D. degree in information engineering from the Politecnico di Bari, Bari, Italy, in 2016 and 2020, respectively.

His Ph.D. activity was focused on innovative photonic and optoelectronic devices for space applications with European Space Agency (ESA) sponsorship in the framework of NPI project (367-2014). Since December 2020, he has been an Assistant Professor with the Politecnico di Bari. His research interests include integrated optoelectronics and photonics devices and systems mainly in the context of biomedical and Space field.

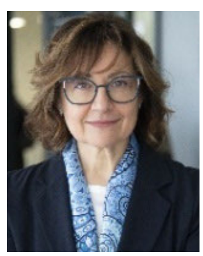

Caterina Ciminelli (Senior Member, IEEE) received the Laurea degree and the Ph.D. in electronic engineering from the Politecnico di Bari, Bari, Italy, in 1996 and 2000, respectively.

From 1999 to 2002, she did industrial research activity on optoelectronic components and subsystems with the Research and Development Division of Pirelli Optical Systems and Cisco Photonics, Italy, before joining the Politecnico di Bari as an Assistant Professor of Electronics in 2002. From 2012 to 2021, she has been an Associate Professor. Since 2021, she has been a Full Professor with the Politecnico di Bari where she is the Scientist responsible for the Optoelectronics Laboratory. Her research interests include integrated optoelectronics and photonics.